

A Density Functional Study of Furofuran Polymers as Potential Materials for Polymer Solar Cells

Xiao-Hua Xie, Wei Shen, Rong-Xing He, and Ming Li*

School of Chemistry and Chemical Engineering, Southwest University, Chongqing 400715, China

*E-mail: liming@swu.edu.cn

Received November 26, 2013, Accepted July 21, 2013

The structural, electronic, and optical properties of poly(3-hexylthiophene) (P3HT) have been comprehensively studied by density functional theory (DFT) to rationalize the experimentally observed properties. Rather, we employed periodic boundary conditions (PBC) method to simulate the polymer block, and calculated effective charge mass from the band structure calculation for describing charge transport properties. The simulated results of P3HT are consistent with the experimental results in band gaps, absorption spectra, and effective charge mass. Based on the same calculated methods as P3HT, a series of polymers have been designed on the basis of the two types of building blocks, furofurans and furofurans substituted with cyano (CN) groups, to investigate suitable polymers toward polymer solar cell (PSC) materials. The calculated results reveal that the polymers substituted with CN groups have good structural stability, low-lying FMO energy levels, wide absorption spectra, and smaller effective masses, which are due to their good rigidity and conjugation in comparison with P3HT. Besides, the insertion of CN groups improves the performance of PSC. Synthetically, the designed polymers PFF1 and PFF2 are the champion candidates toward PSC relative to P3HT.

Key Words : Electronic property, Furofuran, Polymer solar cell, Open-circuit voltage

Introduction

In recent years, more and more researchers have focused on the study of the high efficiency solar cell because of energy crisis and environmental degradation. Traditional solar cells made from high-purity silicon have been commercialized, but their applications are limited because of high cost and weight. Polymer photovoltaic cells with a bulk-heterojunction (BHJ) active layer have attracted attention due to their potentially low cost, light weight, flexibility, and easy manufacturing.¹⁻³ Over past decade, much progress has been made for polymer BHJ, and the polymer BHJ cells have given power conversion efficiency (PCE) greater than 7%,⁴ and even have reached it of 8.3%.⁵ To further improve the device performances, one can develop new device architectures,^{6,7} synthesize new polymer donors^{4,8} and new electron acceptors,⁹⁻¹² or work on both ends.

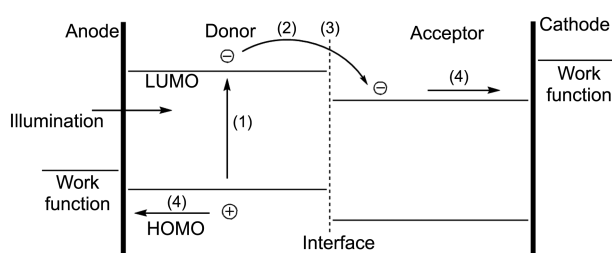
In recent years, developing low-bandgap polymer donors has provided an alternative approach for achieving high PCEs. For the electron donor materials, one most important property is a strong absorption covering a broad spectral region whereas the band gap is less than 2 eV.¹³⁻¹⁶ Another important issue is minimizing the loss processes in the bulk during the exciton and charge transport. The photocurrent generation in the polymer solar cells generally involves in five steps as shown in Scheme 1: (1) absorption of light by the active layer, resulting in creation of excitons, (2) exciton transport to the donor (D)–acceptor (A) interface, (3) dissociation of excitons at the interface of electron donor/acceptor interface, (4) transport of the charges, and (5) charge collection by electrodes. As shown in Scheme 1, polymer

donors play important parts in the photoelectric conversion process, such as obtaining photon influx from the sun, exciton generation and dissociation, and hole transport.

In order to deeply understand the connection between chemical structures and the electronic properties of the donor-acceptor system, and rationally design novel donor-acceptor system, theoretical calculations on them are of importance, especially of some parameters, such as ring current densities, reorganization energies, and charge-transfer integrals are difficult to be obtained from experiments. From the view-point of electronic structure, the donor-acceptor system should have strong electronic coupling whereas the exciton binding energy should be low, and the donor should have large hole mobility. Quantum mechanical calculations on donor-acceptor complexes can provide important information about these properties of the donor-acceptor system. In order to be manageable, the complex issues of a realistic condensed phase environment of the donor-acceptor system are usually neglected in these calculations.

At present, P3HT-PCBM based polymer solar cells (PSCs) (P3HT = regioregular poly(3-hexylthiophene), PCBM = methanofullerene (6,6)-phenyl-C₆₁-butyric acid methyl ester) have achieved an efficiency surpassing 5%.¹⁷ In the past decades, several researchers have investigated the electronic and structural properties of P3HT in theory.¹⁸⁻²⁰ However, to our knowledge, application of PBC-DFT to P3HT has not yet been reported. In addition, led by the work of Bendikov and co-workers, PBC-DFT has been shown to be a very good method to reliably predict the band gaps of conjugated polymers.²¹⁻²⁴

In the present work, we calculated the structural, electronic



Scheme 1. Principle diagram for polymer solar cells.

and optical properties of P3HT to understand the photoelectric conversion process by PBC-DFT method and Marcus theory. Meanwhile, based on furofurans substituted with CN groups, furo[3,4-*b*]furan-2-carbonitrile (FF1), furo[3,4-*b*]furan-3-carbonitrile (FF2), furo[3,2-*b*]furan-3-carbonitrile (FF3) and furo[2,3-*b*]furan-3-carbonitrile (FF4), six polymers, PFF1, PFF2, PFF3a, PFF3b, PFF4a, and PFF4b, were designed to study their potentials toward PSC through comparing their structural, electronic and optical properties with those of P3HT. Furthermore, in order to understand the effects of CN groups on the electronic and optical properties of polymers, we comparatively investigated polymers substituted by CN groups and the unsubstituted ones (1PFa, 1PFc, 2PFc, and PFb) which have been investigated in our previous work.²⁵

This paper is organized as follows. In Section 2, we described the computational methods to obtain the geometries and density topological analyses. In Section 3, the structural, electronic and optical properties of P3HT as well as the experimental observations, and the structural, elec-

tronic and optical properties of the designed polymers were reported. Concluding remarks were given in Section 4.

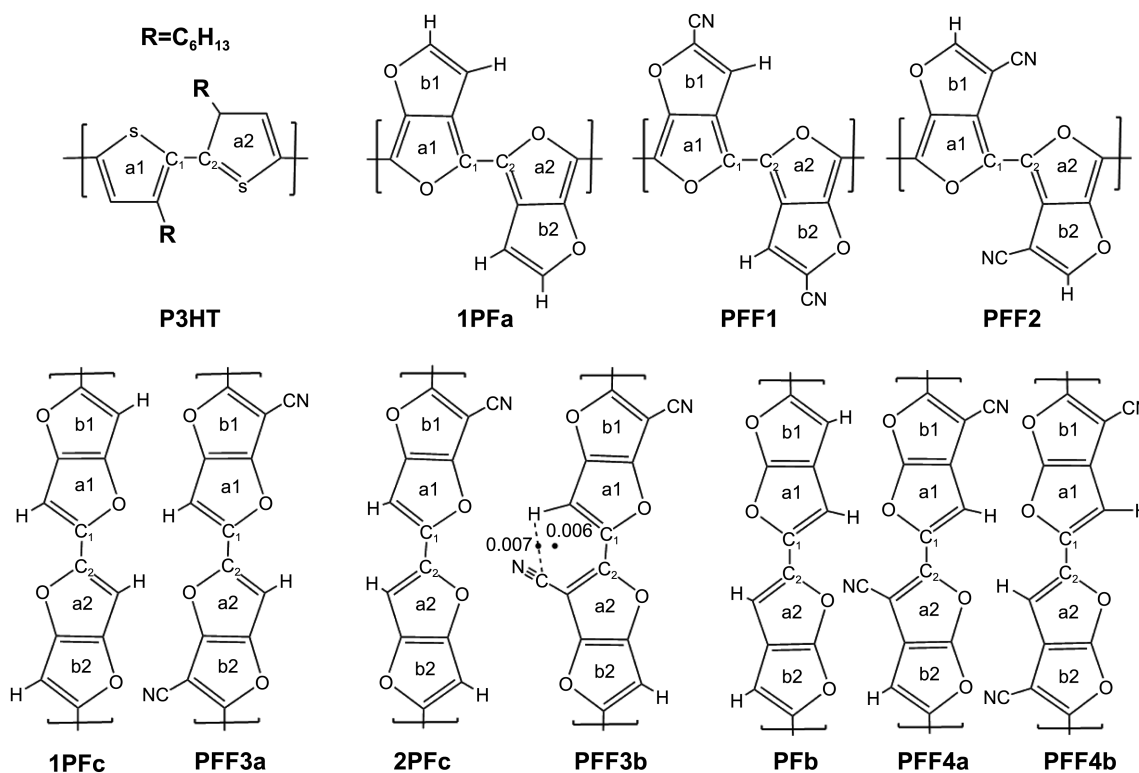
Calculation Methods and Theoretical Details

Density functional theory (DFT) and time-dependent DFT (TD-DFT)²⁶ were used to obtain the qualitative features of all the compounds at B3LYP/6-31G (d) level.^{27,28} All the optimized structures have no imaginary frequencies at the present level. Periodic boundary conditions (PBC)²⁹ method was employed for the block polymers with 6-31G (d) basis set. All the calculations were carried out by Gaussian 03 package.³⁰ In addition, as to the oligomers, density topological analyses were examined by employing atom in molecule (AIM) analyses,³¹ and the nucleus-independent chemical shift (NICS)³² was also calculated at the B3LYP/6-31G (d) level. The NICS method possesses the merit that it allows the evaluation of aromaticity, antiaromaticity, and nonaromaticity of single-ring systems and individual rings in polycyclic systems (local aromaticities).³³ In this work, NICS is defined as the negative of the magnetic shielding at a ring critical point (RCP) and at 1.0 Å above the (RCP) which is gained from the AIM analyses. Furthermore, the bonding characteristics were investigated by natural bond orbital (NBO) theory.³⁴⁻³⁷

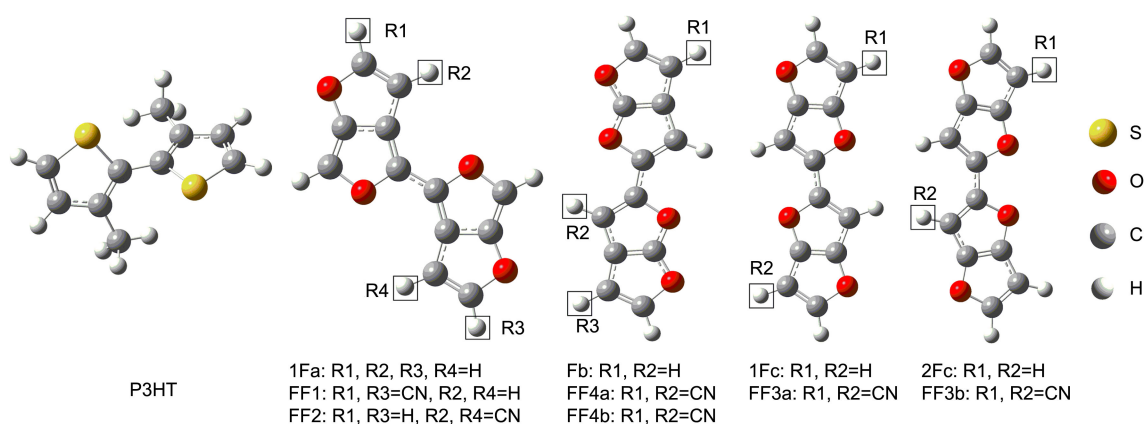
Results and Discussion

P3HT.

Geometry Optimization: The polymer and parent structures of P3HT were displayed in Scheme 2 and Scheme 3,



Scheme 2. Structures and geometrical parameters of polymers.



Scheme 3. Parent structures of calculated polymers.

respectively. The dihedral angle of P3HT is 68° . The central bond (C1-C2) as the π -conjugated bridge as shown in Scheme 2 plays important role in carrier transport process, thus, we investigated the central bond properties of P3HT dimer as shown in Table 1. The bond length (BL) of P3HT is 1.47, and the Wiberg Bond Index (WBI) which measures the π -bond characters is between 1.0 and 2.0, that is to say, the central bond of P3HT displays π -bond characters. In addition, the hybridizations ($SP^{1.76}$) of the carbon atoms (C1, C2) in central bond confirm the results.

Additionally, in order to obtain the charge population analysis of central bond of P3HT, we calculated the properties of bond critical points (BCPs) of central bonds. BCP represents the saddle point between two atoms, is denoted as (3, -1). The charge density $P_{(r)}$ and Laplacian ($\nabla_{\rho}^2(r)$) at the BCP were also listed in Table 1. $P_{(r)}$ and $\nabla_{\rho}^2(r)$ inspect the changes in electronic accumulation,³⁸ and large charge density $P_{(r)}$ (more positive) and Laplacian ($\nabla_{\rho}^2(r)$) (more negative) at BCPs imply large local populations of charges in those bonds. The $\nabla_{\rho}^2(r)$ of P3HT is negative, which indicates that the two atoms in central bond are relatively accumulated due to shared interactions. Moreover, the polymer thermal stability which is critical for PSC in utilization

process is related to the size of bond dissociation energy (BDE). Herein, we calculated the BDE of central bond of P3HT at ground states (BDE^g) and excited states (BDE^e , the vertical excitation of $S_1 \leftarrow S_0$), and listed them in Table 1. The large BDE^g value (525.99 kJ/mol) is between single bond energy (347.7 kJ/mol) and double bond energy (615 kJ/mol) whereas the BDE^e is one half of BDE^g .

Conjugational Properties: Favorable conjugation properties benefit structural stability. To understand the structural stability of P3HT, we investigated the conjugation properties of dimers of P3HT.

Since NICS can distinctly and simply monitor the condition of ring currents, it is widely used to express the aromaticity of molecules. Systems with significantly negative NICS values are aromatic and systems with strongly positive NICS values are anti-aromatic, and non-aromatic cyclic systems should therefore have NICS values close to zero.^{32,39-41} Generally, NICS is computed at a ring center, namely in the position of RCP (NICS (0 Å)), however, it was reported that NICS values computed at 1.0 Å above the RCP (NICS (1.0 Å)) was recommended as being a better measure of π -electron delocalization when compared with that of NICS (0 Å).^{40,42} In the present work, both the NICS (0 Å) and NICS

Table 1. BCP properties, bond lengths (BLs), wiberg bond index (WBI), and electronic configurations for bonding orbitals, and bond dissociation energies (BDE) of central bonds

Polymer	$P_{(r)}$	$\nabla_{\rho}^2(r)$	BL (Å)	WBI	Hybridization	BDE^g (kJ/mol)	BDE^e (kJ/mol)
P3HT	0.27	-0.66	1.47	1.06		525.99	205.52
1PFa	0.30	-0.82	1.43	1.14		583.87	320.59
PFF1	0.30	-0.83	1.42	1.16		587.57	385.21
PFF2	0.30	-0.82	1.43	1.14		586.89	354.23
1PFc	0.30	-0.81	1.43	1.14		580.53	315.34
PFF3a	0.30	-0.82	1.43	1.13		581.38	324.29
2PFc	0.29	-0.80	1.44	1.14		571.51	307.92
PFF3b	0.30	-0.81	1.43	1.15		578.88	348.36
PFb	0.30	-0.81	1.43	1.13		582.24	282.62
PFF4a	0.30	-0.82	1.43	1.14		580.83	330.46
PFF4b	0.30	-0.81	1.43	1.13		581.70	307.98

Table 2. NICS for dimers of all the studied polymers at points 1.0 above (in parenthesis) and at RCPs

Dimer	P3HT	1Fa ²⁵	FF1	FF2	1Fc ²⁵	FF3a	2Fc ²⁵	FF3b	Fb ²⁵	FF4a	FF4b
a1	-11.9 (-8.8)	-13.8 (-9.3)	-13.5 (-9.4)	-14.4 (-9.6)	-10.9 (-8.0)	-11.4 (-8.2)	-11.2 (-8.2)	-11.7 (-8.7)	-11.7 (-8.8)	-10.9 (-8.0)	-10.8 (-7.9)
a2	-11.9 (-8.8)	-13.8 (-9.3)	-13.5 (-9.4)	-14.4 (-9.6)	-10.9 (-8.0)	-11.4 (-8.2)	-11.2 (-8.2)	-12.3 (-9.1)	-11.7 (-8.8)	-11.7 (-8.7)	-10.8 (-7.9)
b1		-8.1 (-6.3)	-9.1 (-6.7)	-8.8 (-6.4)	-11.9 (-8.9)	-12.5 (-9.0)	-11.9 (-8.9)	-12.3 (-8.9)	-11.7 (-8.8)	-12.0 (-8.7)	-12.2 (-8.8)
b2		-8.1 (-6.3)	-9.1 (-6.7)	-8.8 (-6.4)	-11.9 (-8.9)	-12.5 (-9.0)	-11.9 (-8.9)	-11.7 (-8.1)	-11.7 (-8.8)	-11.2 (-7.8)	-12.2 (-8.8)

(1.0 Å) values for monomers and oligomers are calculated and given in Table 2, and the positions of all the rings in the molecular system are shown in Scheme 2.

In Table 2, the NICS values of P3HT indicate that the ring currents in P3HT (more positive) are reducing relative to that in the individual thiophene ring (NICS, -13.9 at B3LYP/6-31G (d) level), which results from the electrons of P3HT delocalizing to the whole molecule, thus forming conjugated systems.

Absorption Spectra: The experimental absorption spectrum of P3HT depicted in Figure 1(a) shows the three absorption bands in the range of 200-650 nm in chloroform solution. The main absorption peak of P3HT is located at approximately 456 nm.⁴³

The simulated absorption spectrum of P3HT-Dimer by TD-DFT/B3LYP method with the same 6-31G (d) basis set was given in Figure 1(b) for comparison, and the effect of the solvent (chloroform) within polarizable continuum model (PCM)⁴⁴ was taken into account during the calculation. The main absorption peak of calculated P3HT-Dimer is located at 269 nm. In comparison with the simulated dimer, the main absorption peak of experiment is red-shifted, which may result from better conjugation of polymer than oligomer. However, the agreements between measured and simulated spectra are well in overall spectral shape.

Moreover, the detailed electronic transitions, absorption wavelengths (λ_{abs}), oscillator strengths (f), and main configuration of dimers were given in Table 1S in Supporting Information. Herein, the $S_1 \leftarrow S_0$ electronic transition coming from HOMO to LUMO (absorption process) is the strongest among the three main electronic transitions. In the process of $S_1 \leftarrow S_0$ electronic transition, charge transfers from conjugation section of homocyclic rings to sulfur atoms as shown in the HOMO and LUMO diagrams of P3HT-Dimer in Figure 1S (in Supporting Information).

The experimental and simulated absorption spectra of P3HT illustrate that P3HT exhibits narrow absorption spectrum which is one of the main hindrances to the further improvement of the efficiencies of P3HT-based devices.

Frontier Molecular Orbitals: In order to harvest the maximum of the photon flux from the sun and get high short-circuit current (J_{SC}), the band gap (E_g) of the polymers should lie between 1.3 and 1.9 eV.⁴⁵ Further, a deep HOMO energy level (-5.2 \rightarrow -5.8 eV) is needed to ensure that the

material is stable toward oxidation from air. Rather, the open-circuit voltage (V_{OC}) of PSC is ultimately limited by the difference between the HOMO of the donor and the lowest unoccupied molecular orbital (LUMO) of the acceptor.^{46,47} In addition, the LUMO(D)-LUMO(A) (L-L) and HOMO(D)-HOMO(A) (H-H) offsets are necessarily larger than 0.3-0.5 eV to guarantee exciton separation. It will be useful to confirm the frontier molecular orbitals (FMOs) of molecules since the relative ordering of the occupied and virtual orbitals provides a reasonable qualitative indication of the excitation properties in the processes of exciton generation and dissociation.

In present work, the structural and electronic properties of polymers were obtained by employing PBC calculation. The FMO energy levels and band gaps of polymers were shown in Figure 2, and the band gap is obtained from the minimum difference between HOMO and LUMO energy levels at a constant k . As shown in Figure 2, the band gap of P3HT is around 1.9 eV, and limits the absorbance to below a wavelength of 650 nm. In addition, the LUMO level, and H-H and L-L offsets of P3HT meet the general requirements for PSC, whereas the HOMO level is higher than the antioxidation level, which is disadvantageous to its antioxidation.

In Figure 2, the HOMO and LUMO levels of P3HT are higher than the measured ones about 0.6-0.7 eV, respectively, and the E_g difference between measurement (1.9 eV) and calculation (2.02 eV) is only 0.12 eV. The different environments between measurement and simulation should be responsible for the slight difference. Additionally, the calculated H-H and L-L offsets are larger than the experimental ones by 0.58, and 0.7 eV, respectively.

In the power conversion efficiency formula: $\eta = V_{OC} \times J_{SC} \times FF/P_m$, the three parameters, V_{OC} , J_{SC} , and FF , determine the solar cell performance directly. The parameter, open-circuit voltage (V_{OC}) formed in the process of carrier transport is widely used to estimate the maximum PCE.¹⁶ As shown in Figure 2, the experimental V_{OC} (P3HT-exp) is obtained when the J_{SC} is equal to zero in J-V curves. With respect to theoretical V_{OC} , it has been described by two models: one is the metal-insulator-metal (MIM) model, which proposes that V_{OC} depends linearly on the work function difference between the two electrodes,⁴⁸ the other model is the HOMO^D-LUMO^A offset model, which describes that V_{OC} changes linearly with the energy level offset between

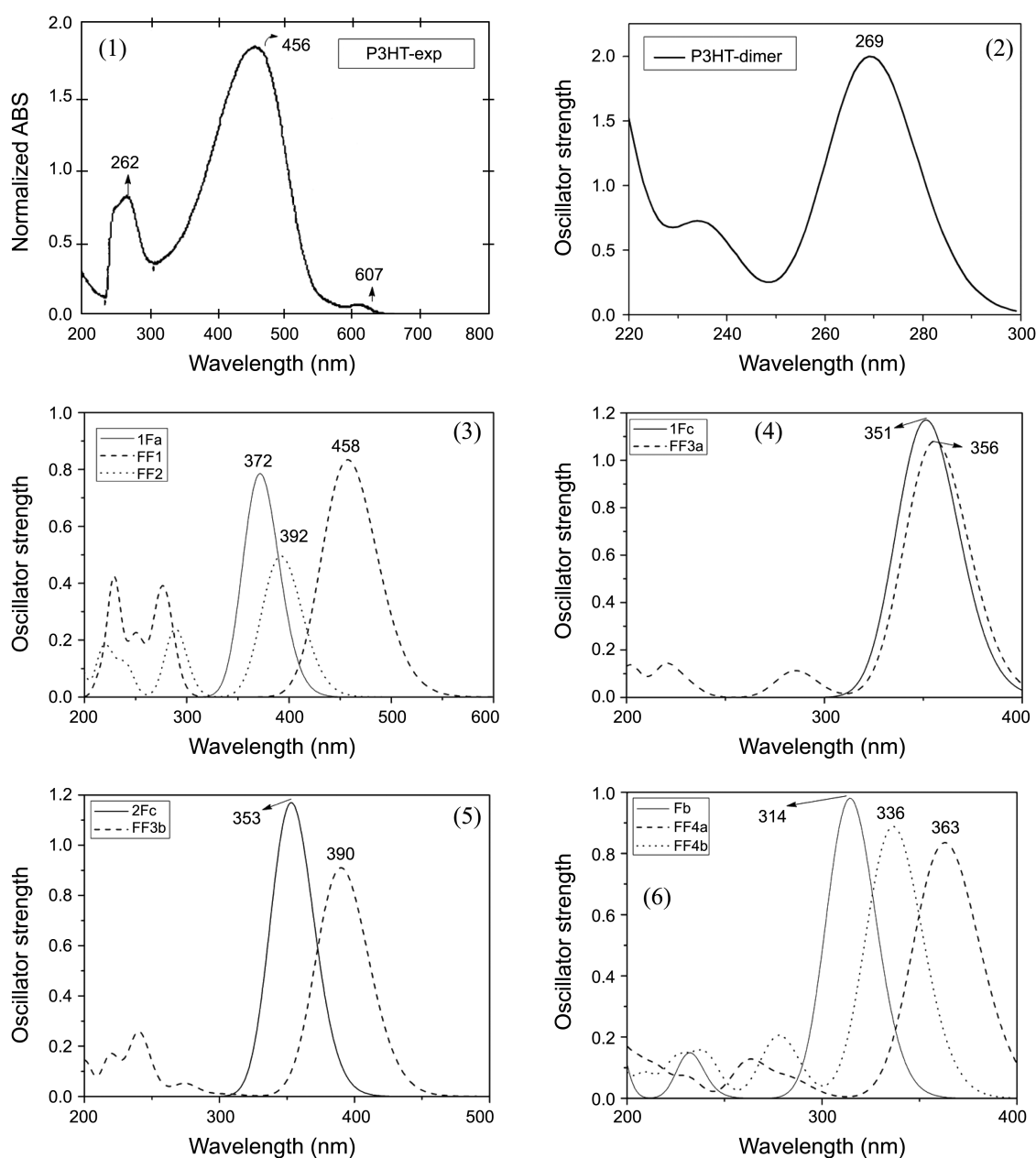


Figure 1. Experimental (1)⁴³ and stimulated absorption spectra (2) of P3HT, and stimulated absorption spectra (3, 4, 5, 6) of investigated derivatives in chloroform solution. (The value of the FWHM is 3000 cm^{-1}).

the HOMO of the donor (D) and the LUMO of the acceptor (A).^{16,49} Recently, Lo *et al.* suggests that V_{OC} is described by a combined MIM model with HOMO^D-LUMO^A offset model. In the model, V_{OC} increases linearly with $\Delta\phi_{electrodes}$ as prescribed by the MIM model when the work function difference ($\Delta\phi_{electrodes}$) between ITO and Al electrode is in the range of -3 and 0 eV. Outside this range, V_{OC} depends on HOMO^D-LUMO^A offset model.⁵⁰ In the paper, we employed the HOMO^D-LUMO^A offset model. The V_{OC} of a conjugated polymer-PC₆₁BM solar cell can be estimated by¹⁶

$$V_{oc} = (1/e)(|E^{Donor} HOMO| - |E^{PCBM} LUMO|) - 0.3V \quad (1)$$

Where e is the elementary charges, E^{PCBM} LUMO is equal to

-4.2 eV (PC₆₁BM), and the 0.3 V is an empirical factor to offset the exciton binding energy.⁵¹ In comparison of the experimental and simulated V_{OC} values, the simulated V_{OC} is lower than the measured one by 0.78 V, which mainly results from the HOMO level difference between simulation and experiment (0.58 eV).

Charge-transfer Properties: In accordance with the band-like theory, the bandwidth (BW) and electron effective mass (m^*) are good parameters for predicting the hole and electron-transporting ability of polymers.⁵²⁻⁵⁴ The effective mass of carrier at the band edge representing mobility was obtained as the square of \hbar multiplied by the reciprocal of the curvature from $E(k)$ with k , and the formulation is defined as

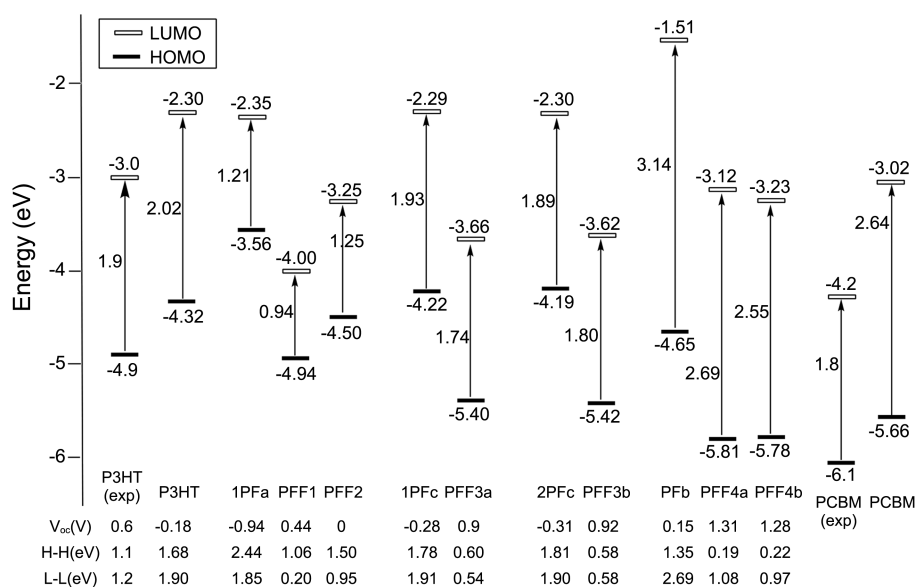


Figure 2. HOMO, LUMO energy levels, and band gaps of polymers (exp represents the values from the experimental measures⁴⁶).

$$\frac{1}{m^*} = \frac{1}{\hbar} \left(\frac{\partial^2 E(k)}{\partial k^2} \right) \quad (2)$$

The kinetic model of mobility (μ) is given by the following formula:

$$\mu = \frac{eT}{m^*} \quad (3)$$

The BW and m^* data are shown in Table 3. According to the band theory, the wider the BW, the smaller the effective mass, and the larger the kinetic model of mobility.⁵⁵ The data in Table 3 investigate that P3HT has wider valence band (2.13 eV) and small m^* (1.48).

Above studies investigate that the electronic and photovoltaic properties are consistent with the experimentally observed properties, and the narrow absorption spectrum in visible region of P3HT is one of its limitations for more favorable performance.

Designed Polymers. Given that the calculations on P3HT gave well explanations to the photoelectric conversion process. We analyzed the electronic, optical, and structural properties of the designed polymers in the following sections as well as the comparison with P3HT.

Geometry Optimization: The structures of all the studied polymers were displayed in Scheme 2. The dihedral angles in the designed oligomers and polymers are close to zero, therefore, these designed compounds are rigid backbones. Rather, the designed polymers have better planarity than P3HT. The parent structures of calculated polymers were shown in Scheme 3. In order to compare with P3HT, we also investigated the π -conjugated bridge in dimers, central bonds (C1-C2), and the data about central bond properties were given in Table 1. In Table 1, the BL values of central bonds in designed dimers are between 1.42–1.44 Å which is shorter than that of P3HT (1.47 Å), and the WBI values of

the designed dimers (between 1.13 and 1.15) are obviously larger than that of P3HT (1.06). In addition, the hybridizations of the carbon atoms (C1, C2) in central bonds of designed polymers illustrate that the p orbital component decreases relative to that in P3HT, which results from the p orbital in designed dimers involving in the central bonds more than that in P3HT. Therefore, the BL, WBI, and hybridization analyses indicate that the central bonds in designed dimers display more π -bond characters than P3HT.

In addition, charge population properties were analyzed as the P3HT. Table 1 listed the properties of BCP in central bonds of designed dimers. The charge densities (more positive) and Laplacian values (more negative) of designed dimers are apparently larger than these of P3HT, which suggests that larger local populations of charges in the central bonds of designed dimers than P3HT.

In a word, as to the designed dimers, the increased p orbital components in bridge bonds lead to large charge accumulations and WBI values, and then lead to short BLs. In other words, the increased charge accumulations strengthen the central bonds, and then increase the central bond energy and strengthen structural stability.

In order to concretely display the structural stability, we calculated the bond dissociation energy (BDE) of the π -conjugated bridge bonds of designed polymers, and listed the data in Table 1. From Table 1, we can see that the BDE° and BDE° values are larger than those of P3HT, respectively, and the results confirm the above analyses that the central bonds of designed polymers are more stable than that of P3HT. What is notable is that the dimers substituted with CN groups have larger BDE than the unsubstituted furofurans, which indicates that CN groups as the electron-withdrawing groups enhance the bridge bonds.

Consequently, the charge accumulations on bridge bonds in designed dimers are larger than those on P3HT, which leads to more stable bridge bonds and structures of designed

Table 3. Band width (eV) and effective mass (m^*)

Polymer	Conduction band		Valence band	
	BW	m^*	BW	$-m^*$
P3HT	1.80	1.62	2.13	1.48
1PFa	1.36	0.70	1.93	0.65
PFF1	1.20	6.98	2.20	0.65
PFF2	1.50	0.96	2.20	0.39
1PFc	2.34	0.26	2.72	0.26
PFF3a	1.01	3.15	1.43	1.42
2PFc	1.50	1.38	1.66	1.38
PFF3b	1.25	3.76	1.58	1.13
PFb	0.57	3.24	0.84	2.84
PFF4a	0.76	5.57	0.87	5.05
PFF4b	0.49	6.56	0.93	4.67

dimers than P3HT, especially of the polymers substituted with CN groups.

Conjugational Properties: As well as P3HT, the calculated NICS values at points 1.0 Å above and at RCPs were listed in Table 2. As shown in Table 2, all the NICS values are negative, therefore, all the studied rings are aromatic. In addition, the NICS values of all *a* rings in 1Fa system (1Fa, FF1, and FF2) are larger (more negative) than these of P3HT, which indicates that the ring currents in *a* rings in 1Fa system are larger than those in P3HT. However, the NICS values in *b* rings in 1Fa system are smaller (more positive) than those in *a* rings of P3HT, which mainly originates from the charges delocalizing along the polymeric axis and *b* rings are farther from the polymeric axis than *a* rings. In other designed systems, all the rings are along the polymeric axis, and all the NICS values from *a* and *b* rings are similar to those of P3HT, that is to say, they have similar ring currents and conjugation to P3HT.

In addition, through investigating the same positions in designed rings, we find that the NICS values in rings with CN groups are apparently larger than those in unsubstituted furofurans, such as the NICS in b1 ring of 1Fa is -6.3, whereas the NICS values in b1 rings in FF1 and FF2 are -6.7 and -6.4, respectively. That is to say, the insertion of CN groups increases the ring currents due to its strong electron-withdrawing strength.

Besides, we also calculated the NICS values of monomers, trimers, and tetramers of designed polymers as shown in Table 2S in Supporting Information. The calculated results indicate that the ring currents in the same positions decrease with the increased polymeric number, which results from the charges delocalizing to the whole molecules, that is to say, the conjugational degree of the oligomers enhances with the increased polymeric number.

In a word, we conclude that the designed polymers are favorable conjugated systems.

Absorption Spectra: The simulated absorption spectra of dimers of designed polymers were presented in Figure 1(b), (d), (e), (f), and the absorption wavelength (λ_{abs}), oscillator

strength (f), and main configuration were listed in Table 1S (see the Supporting Information). The spectra of designed polymers are in the range of 300-400 nm, and they are red-shifted relative to P3HT (200-300 nm). Further, f values of the maximum absorption peaks in designed molecules are larger than these in P3HT. Combining Figure 1 and Table 1S, we can find that the main configurations with the maximum wavelength of the designed molecules belong to single electron transitions and come from HOMO to LUMO mainly assigned to $\pi \rightarrow \pi^*$ transition of the whole molecules.

Moreover, in the four systems, the absorption spectra of dimers substituted with CN groups are red-shifted relative to those of single furofuran dimers (1Fa system: 372 \rightarrow 392, 458 nm; 1Fc system: 351 \rightarrow 356 nm; 2Fc system: 353 \rightarrow 390 nm; Fb system: 314 \rightarrow 336, 363 nm). The absorption spectra of oligomers of polymers substituted with CN groups were depicted in Figure 2S in Supporting Information. As shown in Figure 2S, the absorption spectra are red-shifted with the increased polymeric number in respective systems.

In comparison with simulated absorption spectrum of P3HT, the designed polymers, especially the polymers substituted with CN groups, have more broad and strong absorption spectra, and the absorption peaks lie in smaller energy ranges. The well conjugation of the designed polymers due to well rigidity should be responsible for the improved absorption spectra.

Frontier Molecular Orbitals: The calculated parameters of FMOs were given in Figure 2, and the band structures of polymers substituted with CN are given in Figure 3. As shown in Figure 2, the HOMO and LUMO levels of unsubstituted furofuran polymers are higher than these of P3HT, which are disadvantageous to the antioxidation. Whereas the insertion of CN groups obviously decreases FMO levels and band gaps of substituted polymers, which ascribes to the enhanced charge delocalization and molecular conjugation of designed substituted polymers resulting from the strong electron-withdrawing strength of CN groups. Thus, the substituted polymers with CN groups are the mainly investigated targets.

In Figure 2, the HOMO energy levels of substituted polymers are lower than those of P3HT (simulation), which ascribes to the substituted polymers with better conjugations as the HOMO diagrams shown in Figure 4. In Figure 4, the electronic cloud distributions of HOMOs of all the oligomers localize near the polymeric axis, and the electronic cloud overlap and conjugational degree of oligomers strengthen with increased polymeric number. The LUMO levels of substituted polymers decrease relative to that of P3HT (simulation), and the LUMO diagrams of oligomeric units of designed polymers were exhibited in Figure 5. The rest of HOMO and LUMO diagrams of other oligomers were given in Figure 3S and Figure 4S. Analogously, the electronic cloud distributions of LUMOs of all the oligomers localize near the polymeric axis. Therefore, we can conclude that the hole and electron transport mainly along the polymeric axis, and the designed polymers have better antioxidation properties than P3HT due to lower HOMO energy levels.

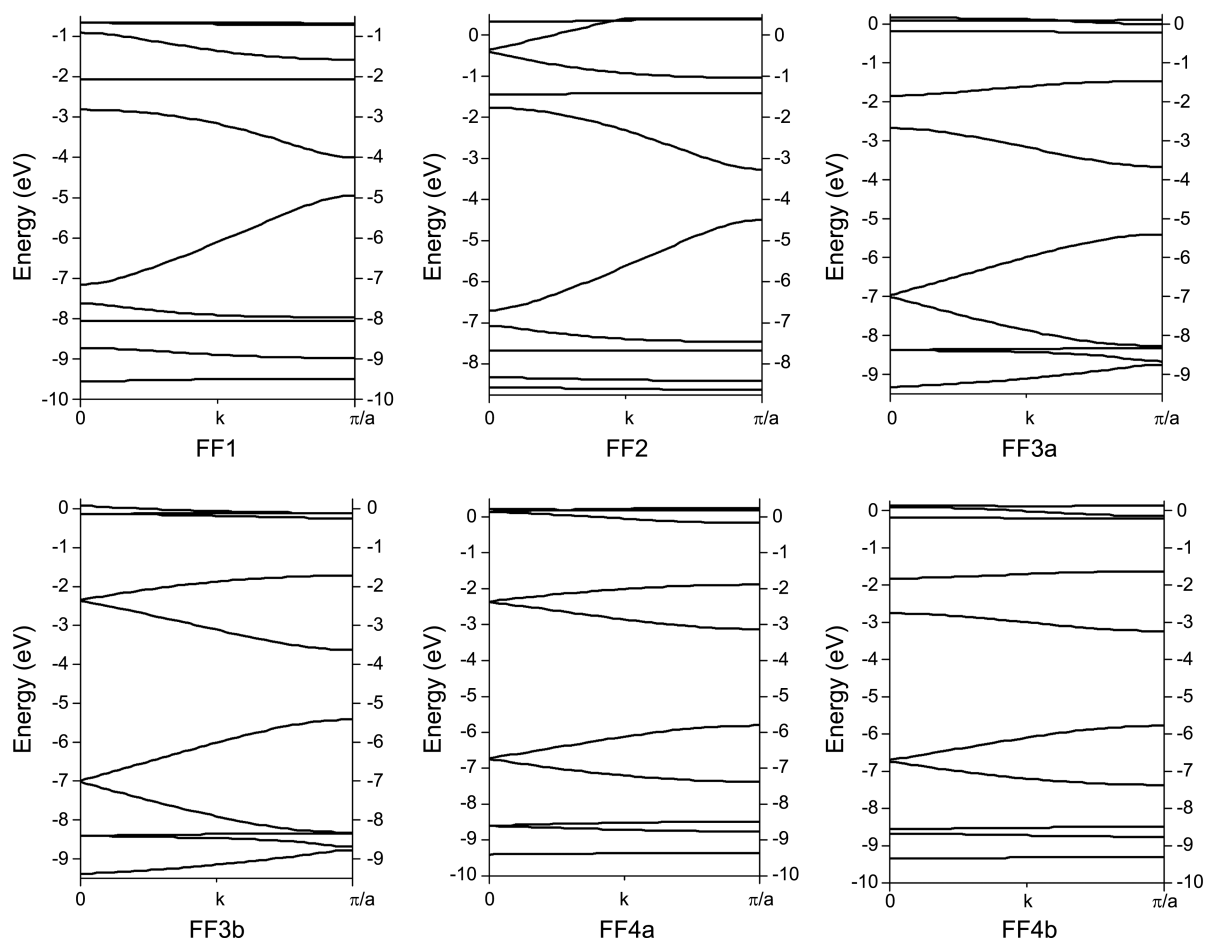


Figure 3. Band structures of polymers substituted with cyano-group.

Though the incorporation of CN groups decrease the FMO energy levels, the band gaps of PFF4a and PFF4b (2.69 and 2.56 eV, respectively) are still larger than that of P3HT. Therefore, only PFF1, PFF2, PFF3a, and PFF4b have smaller band gaps than P3HT for PSC.

In order to understand the properties of the polymers under the circumstance of field, we also calculated the octamers of all the designed polymers in different electric field intensities in terms of relative energy, dipole moment, and charge transfer as listed in Table 3S, and the corre-

sponding diagrams of FMOs were depicted in Figure 4, 3S and Figure 5, 4S. As shown in Figure 4, 3S and Figure 5, 4S, the electronic cloud distributions delocalize along the direction of added field (the direction of arrows). In addition, the electric field reduces the total energy of the octamers with the strengthened intensity of electric field as the relative energy listed in Table 3S. The relative energy means that the optimized octamer energy is regarded as zero eV, and other energies compare with it. The above results indicate that the strong electric field results in large electron delocalization

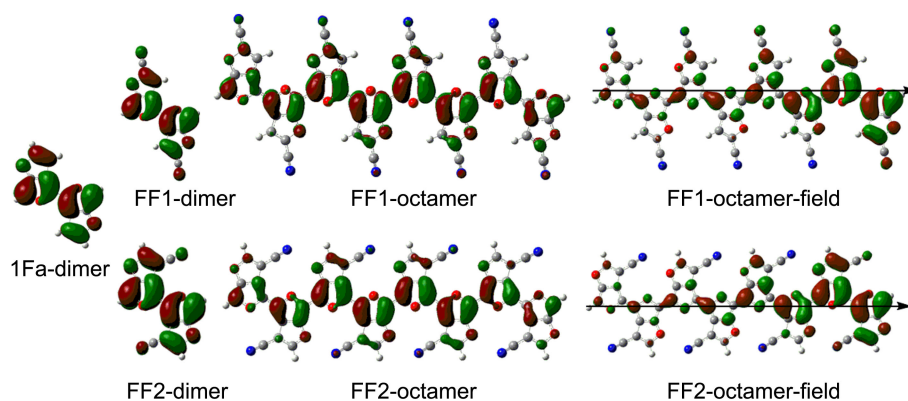


Figure 4. HOMO orbital diagrams for the oligomeric units of 1Fa, FF1, and FF2.

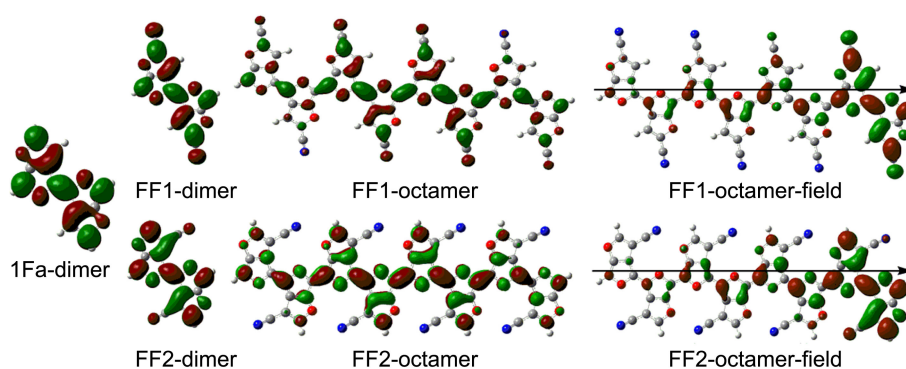


Figure 5. LUMO orbital diagrams for the oligomeric units of 1Fa, FF1, and FF2.

and charge transfer, which suggests that the designed polymers have better charge transfer properties in field.

In addition, the E_g values of designed polymers (smaller than 2.0 eV) are smaller than the simulated structure of P3HT (2.02 eV) by PBC-DFT method. Besides, we also simulated the FMOs of PCBM, and the HOMO, LUMO and E_g energies were exhibited in Figure 2. From Figure 2, we can see that the simulated values are larger than the experimental ones as well as P3HT. Moreover, the simulated HOMO and LUMO diagrams of PCBM were given in Figure 5S.

In order to compare the V_{OC} size with P3HT, we also simulated the V_{OC} of designed polymers by the HOMO^D-LUMO^A offset model. As shown in Figure 2, the polymers substituted with CN groups have larger V_{OC} than that of P3HT in theory due to lower HOMO energy levels. Especially, the V_{OC} values of the PFF3 (PFF3a and PFF3b) and PFF4 (PFF4a and PFF4b) are larger than 0.9 V which are apparently higher than the simulated (-0.18 V) and experimental (0.6 V) ones of P3HT. Besides, considering the basic exciton separation condition (the H^D-H^A and L^D-L^A offsets need be larger than 0.3-0.5 eV), we calculated the H^D-H^A and L^D-L^A offsets between designed polymers (donors) and PCBM (acceptor) and listed the data in Figure 2. The data in Figure 2 indicate that only Fb system don't meet the requirements in theory.

Thus, combining the V_{OC} and FMO offsets, only PFF1, PFF2, PFF3a and PFF3b are promising candidates for PSC due to low-lying FMO energy levels, small band gaps, large V_{OC} , and sufficient H^D-H^A and L^D-L^A offsets for exciton separation relative to P3HT.

Charge-transfer Properties: By the same methods as P3HT, we calculated the band widths and effective masses for designed polymers, and listed the data in Table 3.

From Table 3, we can see that the designed polymers except for PFb systems have smaller valence band widths in comparison of P3HT, especially the polymers 1PFa, PFF1, PFF2, and 1PFc, and these polymers do not have smaller effective masses, but they also have larger valence band widths. In accordance with the above investigations, polymers 1PFa, PFF1, PFF2, and 1PFc have better hole transport properties than P3HT. Moreover, we find in Table 3 that the CN incorporation obviously decreases the effective mass through comparing 1PFa and PFF2.

The above investigations of designed polymers illustrate that polymers PFF1 and PFF2 are promising polymers toward PSC due to their better electronic and photovoltaic properties than P3HT in theory.

Conclusions

In this contribution, we rationalized the experimentally observed properties of P3HT by PBC-DFT method and Marcus theory. The investigations referred to the geometry optimizations, conjugation properties, absorption spectra, frontier molecular orbitals, charge-transfer properties. The simulated results match well with the experimental ones. Based on the same calculated methods, we compared the electronic, optical, and structural properties between the designed polymers and P3HT, and we studied the effects of CN groups on the polymer properties.

In comparison of P3HT, the designed polymers substituted with CN groups have better structural stability, lower FMO energy levels, broader absorption spectra, and larger charge-transfer rates due to their better rigidity and conjugation, and smaller effective mass. In addition, the insertion of CN groups greatly improves the performance of PSC by improving their electronic and structural properties. Synthetically considering the properties of affecting PSC, PFF1 and PFF2 are the champion candidates for PSC due to large open-circuit voltages and smaller effective masses, and sufficient H^D-H^A and L^D-L^A offsets for exciton separation in comparison with P3HT.

In the furofuran systems, CN groups obviously improve FMO energy levels, band gaps, and carrier mobilities, which are significant for improving PCE of PSC. Whether the natures of CN groups are suitable for other system, and whether other groups own such natures, which will be explored in our later works.

Acknowledgments. This work was supported by National Natural Science Foundation of China (Grant No.21073144), and by Ph.D. Programs Foundation of Ministry of Education of China (Grant No. 200806350013), and by Natural Science Foundation Project of CQ CSTC (Grant No. CSTC, 2009BB4104), and by Fundamental Research Funds for the Central Universities (Grant No. XDJK2010B009). We are

grateful to the anonymous referees for their suggestions. And the publication cost of this paper was supported by the Korean Chemical Society.

Supporting Information. HOMO and LUMO orbital diagrams for the oligomeric units of 1Fc and Fb systems, P3HT, PCBM; absorption wavelengths (λ_{abs}), oscillator strengths (f), and main configuration of dimers; negative NICS values of monomers and oligomers; and relative energy, dipole moment, and charge transfer of octamer are provided.

References

- Krebs, F. C. *Sol. Energy Mater. Sol. Cells* **2009**, *93*, 465.
- Krebs, F. C.; Gevorgyan, S. A.; Alstrup, J. *J. Mater. Chem.* **2009**, *19*, 5442.
- Krebs, F. C. *Org. Electron* **2009**, *10*, 761.
- Liang, Y.; Yu, L. *Acc. Chem. Res.* **2010**, *43*(9), 1227-1236.
- Information on http://www.konarka.com/index.php/site/pressreleasedetail/konarkas_power_achieves_world_record_83_efficiency_certification_fr (January 26, 2011).
- Hadipour, A.; De Boer B.; Wildeman J.; Kooistra, F. B.; Hummelen, J. C.; Turbiez, M. G. R.; Wienk, M. M.; Janssen, R. A. J.; Bolm, P. W. M. *Adv. Funct. Mater.* **2006**, *16*, 1897.
- Kim, J. Y.; Lee, K.; Coates, N. E.; Moses, D.; Nguyen, T. Q.; Dante, M.; Heeger, A. J. *Science* **2007**, *317*, 222.
- Bundgaard, E.; Krebs, F. C. *Sol. Energy Mater. Sol. Cells* **2007**, *91*, 954.
- Wienk, M. M.; Wiljan, J. M. K. et al. *Angew. Chem. Int. Ed.* **2003**, *42*, 3371.
- Brabec, C. J.; Cravino, A.; Meissner, D. et al. *Adv. Funct. Mater.* **2001**, *11*, 374.
- Backer, S. A.; Sivula, K.; Kavulak, D. F.; Frechet, J. M. J. *Chem. Mater.* **2007**, *19*, 2927.
- Kooistra, F. B.; Knol, J.; Kastenber, F. et al. *Org. Lett.* **2007**, *9*, 551.
- Svensson, M.; Zhang, F.; Veenstra, S. C. et al. *Adv. Mater.* **2003**, *15*, 988.
- Zhang, F.; Perzon, E.; Wang, X.; Mammo, W.; Andersson, M. R.; Inganäs, O. *Adv. Funct. Mater.* **2005**, *15*, 745.
- Gong, X.; Tong, M.; Xia, Y. et al. *Science* **2009**, *325*, 1665.
- Scharber, M. C.; Mühlbacher, D.; Koppe, M.; Denk, P.; Waldauf, C.; Heeger, A. J.; C. Brabec, J. *Adv. Mater.* **2006**, *18*, 789.
- Irwin, M. D.; Buchholz, B.; Hains, A. W.; Chang, R. P. H.; Marks, T. J. *Proc. Natl. Acad. Sci. USA* **2008**, *105*, 2783.
- Cheung, D. L.; McMahon, D. P.; Troisi, A. *J. Phys. Chem. B* **2009**, *113*, 9393.
- Northrup, J. E. *Phys. Rev. B* **2007**, *76*, 245202/1.
- Guo, J.; Ohkita, H.; Bente, H.; Ito, S. *J. Am. Chem. Soc.* **2010**, *132*, 6154.
- Zade, S. S.; Bendikov, M. *Org. Lett.* **2006**, *8*, 5243.
- Zade, S. S.; Zamoshchik, N.; Bendikov, M. *Acc. Chem. Res.* **2011**, *44*, 14.
- Patra, A.; Wijsboom, Y. H.; Leitun, G.; Bendikov, M. *Org. Lett.* **2009**, *11*, 1487.
- Walker, W.; Veldman, B.; Chiechi, R.; Patil, S.; Bendikov, M.; Wudl, F. *Macromolecules* **2008**, *41*, 7278.
- Xie, X. H.; Shen, W.; Fu, Y. W.; Li, M. *Mol. Simulat.* **2010**, *36*, 836.
- Parr, G.; Yang, W. *Density-functional Theory of Atoms and Molecules*; Oxford New York: University Press; 1989.
- Becke, A. D. *J. Chem. Phys.* **1993**, *98*, 5648-5652.
- Lee, C.; Yang, W.; Parr, R. G. *Phys. Rev. B* **1988**, *37*, 785.
- (a) Fripiat, J. G.; Flamant, I.; Harris, F. E.; Delhalle, J. *Int. J. Quantum Chem.* **2000**, *80*, 856. (b) Bakhshi, A. K.; Liegener, C. M.; Ladik, J.; Seell, M. *Synth. Met.* **1989**, *30*, 79. (c) Bakhshi, A. K.; Ladik, J. *Int. J. Quantum Chem.* **1992**, *42*, 997. (d) Champagne, B.; Mosley, D. H.; Ardré, J. M. *J. Chem. Phys.* **1994**, *100*, 2034. (e) Mosley, D. H.; Fripiat, J. G.; Champagne, B.; Ardré, J. M. *Int. J. Quantum Chem.* **1994**, *S28*, 451. (f) Kudin, K. N.; Scuseria, G. E. *Phys. Rev. B* **2000**, *61*, 16440. (g) Delhalle, J.; Fripiat, J. G.; Harris, F. E. *Int. J. Quantum Chem.* **2002**, *90*, 587. (h) Delhalle, J.; Fripiat, J. G.; Harris, F. E. *Int. J. Quantum Chem.* **2002**, *90*, 1326. (i) Fripiat, J. G.; Delhalle, J.; Harris, F. E. *Chem. Phys. Lett.* **2006**, *422*, 11. (j) Hirata, S. *PCCP* **2009**, *11*, 8397.
- Frisch, M. J.; Trucks, G. W.; Schlegel, H. B.; Scuseria, G. E.; Robb, M. A.; Cheeseman, J. R.; Montgomery, J. A.; Pople, J. A. et al. (2003) Gaussian 03, Revision A.01. Gaussian, Inc, Pittsburgh PA.
- Bader, R. F. W. *Atoms in Molecules, A Quantum Theory: International Series of Monographs in Chemistry*; Vol. 22, Oxford, U.K.: Oxford University Press; 1990.
- Schleyer, P. v. R.; Maerker, C.; Dransfeld, A.; Jiao, H.; van Eikema Hommes, N. J. R. *J. Am. Chem. Soc.* **1996**, *118*, 6317.
- Shen, W.; Li, M.; He, R. X.; Zhang, J. S.; Lei, W. *Polymer* **2007**, *48*, 3912.
- Carpenter, J. E.; Weinhold, F. *J. Mol. Struct. (THEOCHEM)* **1988**, *46*, 41.
- Reed, A. E.; Curtiss, L. A.; Weinhold, F. *Chem. Rev.* **1988**, *88*, 899.
- Foster, J. P.; Weinhold, F. *J. Am. Chem. Soc.* **1980**, *102*, 7211.
- Reed, A. E.; Weinstock, R. B.; Weinhold, F. *J. Chem. Phys.* **1985**, *83*, 735.
- Zheng, W. X.; Wong, N. B.; Wang, W. Z.; Zhou, G.; Tian, A. *J. Phys. Chem. A* **2004**, *108*, 97.
- Fu, Y. W.; Shen, W.; Li, M. *Polymer* **2008**, *49*, 2614.
- Schleyer, P. v. R.; Jiao, H.; van Eikema Hommes, N. J. R.; Malkin, V. G.; Malkina, O. *J. Am. Chem. Soc.* **1997**, *119*, 12669.
- Schleyer, P. v. R.; Jiao, H. *Pure Appl. Chem.* **1996**, *68*, 209.
- Schleyer, P. v. R.; Manoharan, M.; Wang, Z. X.; Kiran, B.; Jiao, H. J.; Puchta, R.; van Eikema Hommes, N. J. R. *Org. Lett.* **2001**, *3*, 2465.
- Chen, T.; Wu, X.; Rieke, R. D. *J. Am. Chem. Soc.* **1995**, *117*, 233.
- Tomasi, J.; Mennucci, B.; Cammi, R. *Chem. Rev.* **2005**, *105*, 2999.
- Kroon, R.; Lenens, M.; Hummelen, J. C.; Blom, P. W. M.; de Boer, B. *Polym. Rev.* **2008**, *48*, 531.
- Brabec, C. J.; Cravino, A.; Meissner, D.; Sariciftci, N. S.; Fromherz, T.; Rispens, M. T.; Sanchez, L.; Hummelen, J. C. *Adv. Funct. Mater.* **2001**, *11*, 374.
- Koster, L. J. A.; Mihaileti, V. D.; Ramaker, R.; Blom, P. W. M. *Appl. Phys. Lett.* **2005**, *86*, 123509/1-123509/3.
- Mihaileti, V. D.; Blom, P. W. M.; Hummelen, J. C.; Rispens, M. T. *Appl. Phys.* **2003**, *94*, 6849.
- Bauschlicher, C. W., Jr.; Lawson, J. W. *Phys. Rev. B* **2007**, *75*, 115406/1-115406/6.
- Lo, M. F.; Ng, T. W.; Liu, T. Z.; Roy, V. A. L.; Lai, S. L.; Fung, M. K.; Lee, C. S.; Lee, S. T. *Appl. Phys. Lett.* **2010**, *96*, 113303/1-113303/3.
- Bredas, J. L.; Beljonne, D.; Coropceanu, V.; Cornil, J. *Chem. Rev.* **2004**, *104*, 4971.
- Haddon, R. C.; Siegrist, T.; Fleming, R. M.; Bridenbaugh, P. M.; Laudise, R. A. *J. Mater. Chem.* **1995**, *5*, 1719.
- Cornil, J.; Calbert, J. P.; Brédas, J. L. *J. Am. Chem. Soc.* **2001**, *123*, 1250.
- Cheng, Y. C.; Silbery, R. J.; da Silva Filho, D. A.; Calbert, J. P.; Cornil, J.; Brédas, J. L. *J. Chem. Phys.* **2003**, *118*, 3764.
- Zhu, J. G.; Zheng, W. X.; Zheng, J. G.; Sun, X. S.; Wang, H. T. *Solid Physics*, Science Press, 2005.